ARTICLE

Biopolymers WILEY

The reversible low-temperature instability of human DJ-1 oxidative states

Tessa Andrews[1] | Javier Seravallic[2] | Robert Powers[1,3,4]

[1]Department of Chemistry, University of Nebraska-Lincoln, Lincoln, Nebraska, 68588-0304, USA

[2]Department of Biochemistry, University of Nebraska-Lincoln, Lincoln, Nebraska, 68588-0664, USA

[3]Redox Biology Center, University of Nebraska-Lincoln, Lincoln, Nebraska, 68588-0664, USA

[4]Nebraska Center for Integrated Biomolecular Communication, University of Nebraska-Lincoln, Lincoln, Nebraska, 68588-0304, USA

Correspondence
Robert Powers, Department of Chemistry, University of Nebraska-Lincoln, 722 Hamilton Hall, Lincoln, NE 68588-0304,
Email: rpowers3@unl.edu

Funding information
Nebraska Center for Integrated Biomolecular Communication, Grant/Award Number: P20GM11312; National Institutes of Health, Grant/Award Number: RR01546

Abstract

DJ-1 is a homodimeric protein that is centrally involved in various human diseases including Parkinson disease (PD). DJ-1 protects against oxidative damage and mitochondrial dysfunction through a homeostatic control of reactive oxygen species (ROS). DJ-1 pathology results from a loss of function, where ROS readily oxidizes a highly conserved and functionally essential cysteine (C106). The over-oxidation of DJ-1 C106 leads to a dynamically destabilized and biologically inactivated protein. An analysis of the structural stability of DJ-1 as a function of oxidative state and temperature may provide further insights into the role the protein plays in PD progression. NMR spectroscopy, circular dichroism, analytical ultracentrifugation sedimentation equilibrium, and molecular dynamics simulations were utilized to investigate the structure and dynamics of the reduced, oxidized ($C106-SO_2^-$), and over-oxidized ($C106-SO_3^-$) forms of DJ-1 for temperatures ranging from 5°C to 37°C. The three oxidative states of DJ-1 exhibited distinct temperature-dependent structural changes. A cold-induced aggregation occurred for the three DJ-1 oxidative states by 5°C, where the over-oxidized state aggregated at significantly higher temperatures than both the oxidized and reduced forms. Only the oxidized and over-oxidized forms of DJ-1 exhibited a mix state containing both folded and partially denatured protein that likely preserved secondary structure content. The relative amount of this denatured form of DJ-1 increased as the temperature was lowered, consistent with a cold-denaturation. Notably, the cold-induced aggregation and denaturation for the DJ-1 oxidative states were completely reversible. The dramatic changes in the structural stability of DJ-1 as a function of oxidative state and temperature are relevant to its role in PD and its functional response to oxidative stress.

KEYWORDS
DJ-1, dynamics, NMR, Parkinson disease, structural biology

1 | INTRODUCTION

The function of a protein is intrinsically linked to its structure and dynamics, which, in turn, have influence on its thermal stability.[1]

Under the right physiological condition, a polypeptide chain will rapidly and efficiently fold into a correct three-dimensional (3D) ensemble of structures.[2] The interatomic interactions between individual amino acid residues guide this folding process. The resulting set of

electrostatic and hydrophobic interactions determine the thermodynamic and kinetic stability of the final protein conformation.[3,4] The overall stability of this structure is tenuous despite the relatively large number of energetic interactions. Simply, the free energy (ΔG) of properly folded proteins is relatively small, only on the order of a few kcal/mole.[5,6] Since free energy depends on temperature, a delicate balance between structural stability and instability occurs, which is occasionally disrupted and protein misfolding or denaturation can occur. Proteins are typically stable at physiological temperatures (i.e., 37°C) and only begin to unfold and denature as the temperature rises and reaches their melting temperature (T_m). Protein denaturation often leads to aggregation where there is a clearly established competition between protein folding and aggregation.[7] Importantly, unfolded, misfolded, and aggregated proteins result in a loss in function and tend to be toxic to the cell,[8] which requires several systems to prevent (i.e., chaperones or heat-shock proteins),[9] or remove (i.e., ubiquitin-proteosome system) these misfolded proteins.[10]

The free energy stability curve for protein folding crosses zero at temperatures both significantly above and below physiological temperature. Thus, low temperature or cold denaturation of a protein is of equal interest as thermal denaturation,[11] but has seen limited investigation since most cold denaturation of proteins occur at temperatures much lower than the freezing point of water.[12] Cold denaturation proceeds through the same unfolding process as high-temperature protein denaturation, but it likely follows a distinct energetic pathway. Regardless, both denaturation methods effectively reduce protein stability, increase the likelihood of protein aggregation, and lead to a loss of function. These misfolded proteins can accumulate and form large fibrillar or amyloid aggregates that can then lead to the formation of visible plaques and cellular tangles that cause cell death.[13] Thus, protein misfolding plays important roles in a variety of human diseases such as type 2 diabetes, cataracts, atherosclerosis, Alzheimer disease, and Parkinson disease (PD).

PD is a destructive neurodegenerative disease that is believed to be caused by several factors, including environmental toxins, aging, and genetic mutations.[14] The exact mechanism of PD progression is unknown but it is brought about by the death of dopaminergic neurons in the substania nigra.[15] The aggregation of α-synuclein and the formation of Lewy bodies are important factors associated with PD neuronal cell death.[16] To date, several gene mutations have been identified that are believed to play a role in PD.[17] These genes encode for proteins such as parkin, leucine-rich repeat kinase 2 (LRRK2), phosphatase and tensin homolog (PTEN)-induced putative kinase 1, and DJ-1.

First reported in 1997 as an oncogene,[18] mutations in human DJ-1 has since been identified in patients with early-onset PD.[19] DJ-1 is a highly conserved and ubiquitous 20 kDa (189 aa) protein encoded by the *PARK7* gene.[17,20,21] The protein is a symmetric homodimer, where each monomer forms a flavodoxin-like Rossmann-fold (Figure 1).[22–25] DJ-1 is a member of the DJ-1/ThiJ/PfpI superfamily and it is distributed throughout the body, which includes the central nervous system (CNS).[26–28] DJ-1 is localized in the cytoplasm, nucleus and mitochondria and can exert specific functions in different compartments.[29] DJ-1 is believed to be involved in multiple cellular processes,
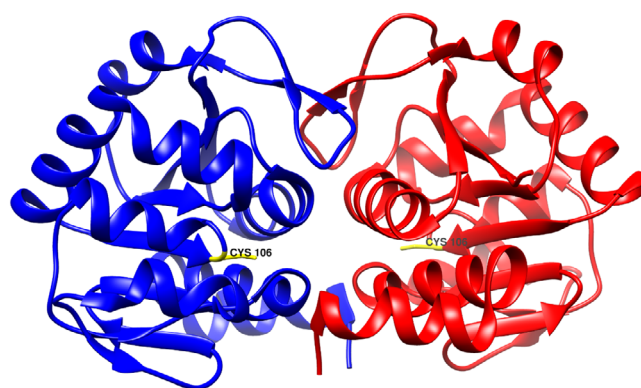
FIGURE 1 Ribbon representation of the DJ-1 homodimer. One homodimer is shown in blue, the other in red. C106 is labeled and colored yellow.

such as the control of ROS,[30,31] transcription regulation[32] and glucose modulation.[33] Furthermore, overexpression of DJ-1 leads to cytoprotection against oxidative stress and under-expression causes oxidative stress-induced cell death.[34–37] In fact, five different signaling pathways have been identified that are controlled by DJ-1 in response to oxidative stress.[21,38–45] However, the molecular mechanism(s) of DJ-1-mediated cytoprotection are not well-understood.

One of DJ-1's three cysteines, C106, is highly conserved and is a key regulator of its cytoprotective role.[31,46–48] Mutations at C106 cause loss of function,[31,46–48] which may result from a decrease in protein stability, a misfolded or denatured protein, or protein aggregation.[49,50] C106 can also be readily oxidized to the sulfenate, sulfinate, and sulfonate forms. These unique oxidation states have been seen in PD patients.[26,51] Oxidation of C106 to the sulfinate ($C106\text{-}SO_2^-$, oxidized) and sulfonate ($C106\text{-}SO_3^-$, over-oxidized) forms cause structural instability.[46,47] The monoxidation of C106 to form the sulfenic acid group is required for the neuroprotective activity of DJ-1 in the mitochondria.[30] We have previously demonstrated that an increase in dynamics is a source of this structural instability[52–54] despite the fact that the overall structural fold remains basically intact.[46,55–57] However, it is unknown whether these DJ-1 oxidative states cause PD progression or are just a consequence of the neurodegenerative disease. An analysis of DJ-1 dynamics and structural stability as a function of oxidative state and temperature may provide insights into the protein's role in PD progression. Toward this end, nuclear magnetic resonance (NMR) spectroscopy, circular dichroism (CD), analytical ultracentrifugation (AUC) and molecular dynamics (MD) simulations were used to characterize the structure and dynamics of the reduced, oxidized and over-oxidized forms of DJ-1 over a range of temperatures (5°C to 37°C). The reduced, oxidized, and over-oxidized forms of DJ-1 exhibited three distinctly different behaviors as the temperature decreased. In all cases, DJ-1 appears to undergo partial or complete cold-induced aggregation at moderately low temperatures that is completely reversible. Notably, the oxidation state of DJ-1 was correlated with these temperature-dependent

changes where a higher oxidation state aggregated quicker as the temperature was lowered.

2 | MATERIALS AND METHODS

2.1 | Protein expression and purification

Unlabeled DJ-1 was expressed from *E. coli* BL21 in Luria-Bertani (LB) broth media and uniformly ^{15}N labeled DJ-1 was expressed in minimal M9 media supplemented with ^{15}N ammonium chloride. Both media were supplemented with 0.1 g/L ampicillin. Cells were incubated at 37°C overnight. Expression of DJ-1 was induced at OD_{600} 0.6–1.0 by the addition of 1 mM isopropyl β-D-thiogalactopyranoside (IPTG). After 5 h of incubation at 37°C, cells were harvested by centrifugation at 5,000 rpm and 5°C and resuspended in 25 mL of wash buffer (50 mM HEPES, 300 mM KCl, 20 mM imidazole) at pH 7.5. About 10–15 mg/mL lysozyme was added to the buffer, and cells were lysed by rocking at room temperature for 30 min followed by repeated sonication (i.e., 10 times for 10 s). Lysates were centrifuged at 4,000 rpm for 20 min at room temperature to remove cell debris. The supernatant was added to a Ni^{2+} affinity column (Sigma-Aldrich, St. Louis, MO) that was preconditioned with wash buffer. The hexahistidine tagged DJ-1 was purified using the Ni^{2+} metal affinity column based on standard procedures. An elution buffer (50 mM HEPES, 300 mM KCl, 500 mM imidazole) was used to remove DJ-1 from the column. Eluted fractions were dialyzed for 4 h at room temperature using a 10 kDa molecular-weight snakeskin tubing (Thermo-Scientific Scientific, Waltham, MA) against a storage buffer (25 mM HEPES, 100 mM KCl) to remove excess imidazole. Samples were then placed in a − 80°C freezer until needed.

2.2 | Preparation of DJ-1 samples for CD, AUC, and NMR experiments

Unlabeled DJ-1 samples were dialyzed overnight at 4°C against either 10 mM sodium phosphate at a pH of 7.2 (CD), 5 mM Tris and 100 mM KCl buffer at pH 7.5 (AUC), or 25 mM 2-(N-morpholino)ethanesulfonic acid (MES) buffer with 100 mM KCl (NMR). Either 2 mM tris (2-carboxyethyl) phosphine (TCEP, CD) or DTT (AUC, NMR) was added to the reduced DJ-1 sample. The oxidized and over-oxidized samples were prepared by the addition of hydrogen peroxide (H_2O_2) at 1:8 and 1:100 molar ratios of protein:H_2O_2, respectively. Samples were incubated on ice for 45 min and 4 h, respectively. Both oxidized samples then underwent a buffer exchange to remove excess H_2O_2 and all samples were concentrated using a stirred cell to a final concentration of 10–2.5 μM (CD), approximately 1 mg/mL (AUC), or approximately 1 mM (NMR), which was consistent with previously published data.[32] The NMR samples were transferred to 5 mm Shigemi tubes for NMR analysis. The reduced, oxidized, and over-oxidized forms of DJ-1 were verified by intact mass. Please see the supplemental information for a detailed description of the sample preparation and intact mass protocols.

2.3 | CD experiments

All CD experiments were collected on a Jasco815 spectrometer (Jasco Inc., Easton, MD) in a 1 mm pathlength quartz cuvette. Spectra were collected in continuous scanning mode at a rate of 20 nm/min. Each spectrum was collected in four accumulated scans with 1 nm bandwidth and a data integration time of 1 s, in accordance with the previously collected data.[58] Spectra were collected at 5°C and 37°C for the reduced, oxidized and over-oxidized forms of DJ-1. All CD spectra were processed using the Jasco Spectra Manager software and the Spectra Analysis feature. All spectra were smoothed using the "Adaptive Smoothing" function. The secondary structure prediction based on the CD spectra was completed using the online webserver Capito (https://capito.uni-jena.de).[59]

2.4 | Analytical ultracentrifugation experiments

All AUC sedimentation equilibrium experiments were collected at 20°C or 5°C on a Beckman Coulter XL-1 analytical ultracentrifuge (Beckman-Coulter, Indianapolis, IN), and at four rotor speeds (3,000, 4,000, 8,000 and 12,000 rpm). At each speed, the absorption at 270 nm was measured as a function of radial position. The AUC datasets were fit to a single molecular-weight using a global fitting model without weighting. The results were analyzed with the Beckman application for Origin v 6.0 (https://www.originlab.com/), Sedfit, and Sedphat.[60] Please see the supplemental information for a detailed description of the AUC protocols.

2.5 | NMR experiments

All NMR experiments were collected on a 700 MHz Bruker Advance III spectrometer equipped with a 5 mm QCI-P probe with cryogenically cooled carbon and proton channels. Two-dimensional (2D) ^1H-^{15}N HSQC experiments were collected for the three oxidative states of DJ-1 at various temperatures using the "hsqcetf3gpsi" pulse program. The spectra were collected at 37°C, 30°C, 25°C, 20°C, 15°C, 10°C, and 5°C using 16 dummy scans, 4 scans per spectra and a sweep width of 11,160 Hz and 2,048 data points in the proton dimension and a 2,839 Hz sweep width with 256 data points in the nitrogen dimension. Each spectrum was processed in NMRPipe[61] with sine-bell window function and one zero fill in both dimensions. Peak picking, chemical shift analysis and linewidth determination were performed using NMRFAM-Sparky.[62] Chemical shift perturbations (CSPs) and linewidth changes were measured relative to the 2D ^1H-^{15}N HSQC spectra at 25°C and the previously reported backbone assignments (BMRB ID 17507) that were acquired at 25°C.[56] The weighted average CSP was calculated according to the equation:

$$CSP = \sqrt{\frac{\left(\frac{\delta_N}{5}\right)^2 + \delta_H^2}{2}},$$

where δ_N and δ_H are the changes in the ^{15}N and ^{1}H chemical shifts, respectively.

2.6 | Molecular dynamics simulations

All MD simulations were run on a computer cluster consisting of 7232 Intel Xeon cores in 452 nodes with 64GB RAM per node within the Holland Computing Center (HCC). When possible, GPU cores were used to increase computing power. All MD simulations were conducted using the GROMACS software.[63] All MD simulations used the DJ-1 structure corresponding to PDB ID 2OR3[64] and previously published partial charges[65] for the oxidized and over-oxidized forms of DJ-1 (Table S1). A series of validation steps were completed to ensure the CSD (sulfinic acid) and OCS (sulfonic acid) parameterizations were correct using PDB files (Table S2), which contain either CSD or OCS residues. Order parameters were calculated from the atom coordinates from the entire MD simulation using the isotropic reorientational eigenmode dynamics (iRed) software.[66] Please see the supplemental information and a GitHub repository (https://git.unl.edu/powers-group/2022-biopolymers-supplemental) for a detailed description of the MD protocols.

3 | RESULTS

3.1 | Intact mass deconvolution substantiate DJ-1 oxidation states

The reduced, oxidized, and over-oxidized forms of DJ-1 eluted at 36.5 min in the LC–MS gradient. The average spectrum between 36.2 and 36.7 min was deconvoluted, which resulted in a major species of average molecular-weight (AMW) of 21,283 ± 1 Da for the reduced form of DJ-1, 21,316 ± 1 for the oxidized form of DJ-1, and 21,396 for the over-oxidized form of DJ-1. The AMW of DJ-1 predicted from the sequence for the ^{13}C- and ^{15}N-labeled sequence of the protein is 21,293 g/mol. The 10 Da deviation is expected for a low resolution quadrupole ion separation (~470 ppm). However, since the result was consistent with several separate injections it is likely that the deviation comes from incomplete isotope enrichment (99.3% enrichment assuming no mass error). The oxidized DJ-1 sample showed an increase in mass of 33 Da, which is consistent with the expectation of 2 O atoms incorporated into C106. In contrast, the over-oxidized DJ-1 sample showed a mass increase of 113 Da, consistent with the addition of 7 O atoms to DJ-1. The most likely explanation is that C47 and C54 underwent dioxidation events while C106 incorporated 3 O atoms. Furthermore, the second treatment of the oxidized DJ-1 sample with a 10-fold excess of H_2O_2 for ~24 h at 4°C produced a species which deconvoluted to an AMW of 21,330, consistent with the

incorporation of 3 O atoms (*data not shown*). The deconvolution results for the reduced, oxidized, and over-oxidized samples are shown in Figure S1. While these results do not exclude oxidation at other amino acid positions within DJ-1, the most likely explanation is that C106 is the single *locus* of oxidation under these conditions.

3.2 | CD spectra indicate no secondary structural changes in DJ-1 oxidative states at low temperature

CD is routinely used to measure the percentage of each secondary structure element present in a protein structure.[35] In this regard, structural changes that occur as a result of changes in temperature or oxidative state can be easily quantified.[36] Based on the high-resolution (1.1 Å) X-ray structure of wild-type (WT) human DJ-1 (PDB ID 1P5F),[25] approximately 42% of the residues in DJ-1 are part of an α-helix, 21% comprise β-strands, and 37% of the residues are in random coils. The analysis of the CD spectra of DJ-1 indicates that the reduced and oxidized forms of the protein were structurally stable at both 5°C and 37°C (Figure 2) and generally consistent with the X-ray structure (Table 1). A close examination of the CD spectra indicated some subtle differences between the reduced and oxidized forms of DJ-1. Specifically, there appears to be a more pronounced dip for the oxidized forms at ~210 nm and a more pronounced dip at ~225 nm for the reduced form. However, these differences had minimal impact on the predicted secondary structure composition of the reduced form compared to the oxidized and over-oxidized forms. Importantly, there were no discernable differences in the CDs when the spectra at 5°C and 37°C were directly overlayed for either the reduced, oxidized, or over-oxidized forms of DJ-1.

3.3 | AUC sedimentation equilibrium experiments indicate low temperature and oxidation induce DJ-1 oligomerization

AUC sedimentation equilibrium experiments are a vital tool for the quantitative analysis of the oligomeric states of biomolecules.[38] The AUC data at 20°C suggest that the oxidative states of DJ-1 sedimented with drastically different molecular-weights compared to the reduced form (Figure 3). The reduced form of DJ-1 exhibited a molecular-weight of approximately 20 kilodaltons (kDa). Conversely, the oxidized form of DJ-1 had a molecular-weight of approximately 63 kDa. The over-oxidized form of DJ-1 displayed an even higher molecular-weight of 104 kDa. The relative masses of the reduced, oxidized, and over-oxidized forms of DJ-1 at 20°C was 1:3:5.

Surprisingly, the AUC sedimentation equilibrium data at 5°C showed a relatively consistent molecular-weight between the three oxidative states of DJ-1. The reduced form of DJ-1 sedimented with a molecular-weight of 112 kDa. Similarly, the oxidized and over-oxidized forms of DJ-1 exhibited apparent molecular-weights of 138 kDa and 104 kDa, respectively. The over-oxidized form of DJ-1 exhibited the same molecular-weight at both 20°C and 5°C; whereas,
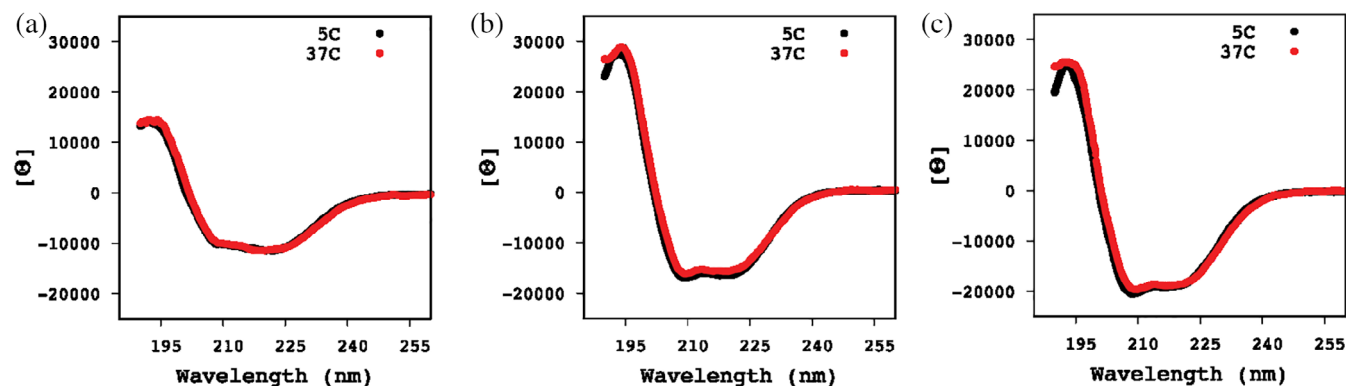
FIGURE 2　CD spectra of the (a) reduced, (b) oxidized, and (c) over-oxidized forms of DJ-1 at 5°C (black) and 37°C (red).

TABLE 1　Summary of CD and AUC analysis.

	Reduced DJ-1	SO$_2^-$ DJ-1	SO$_3^-$ DJ-1	WT DJ-1[a]
37°C or 20°C[b]				
% α-helix	35.2	41.8	39.4	42
% β-strand	10.0	13.1	11.5	21
% Random coil	54.8	45.2	48.9	37
Apparent MW (kDa)	20 ± 2	63 ± 6	104 ± 22	20
5°C				
% α-helix	35.2	44.6	39.4	42
% β-strand	10.0	13.3	11.5	21
% Random coil	54.8	42.1	48.9	37
Apparent MW (kDa)	112 ± 10	138 ± 17	104 ± 13	20

[a]values calculated for the X-ray structure of WT human DJ-1 (PDB ID 1P5F),[25] the listed molecular-weight is for the DJ-1 monomer.
[b]CD spectra were measured at 37°C and AUC was measured at 20°C.

the molecular-weight of the oxidized form doubled, and the reduced form increased by a factor of five. Important, fitting the AUC data with Origin, Sedfit or Sedphat yielded the same results.[67]

3.4 | 2D ^{1}H-^{15}N HSQC spectra of DJ-1 oxidative states suggests low-temperature-induced reversible aggregation and cold denaturation

2D ^{1}H-^{15}N HSQC spectra were acquired at temperatures ranging from 5°C to 37°C in 5-degree increments to further characterize the structural and dynamic differences between the DJ-1 oxidative states. A comparison of the temperature-dependent 2D ^{1}H-^{15}N HSQC spectra for the reduced form of DJ-1 indicates intense line broadening occurred as the temperature was lowered (Figure 4a–c and S2). At 37°C, 134 of the 180 residues were visible and assignable. However, many peaks broadened out into the baseline and were no longer detectable as the temperature decreased. At 5°C, only 21 peaks could be reliably assigned. Importantly, the observable peaks did not

collapse to the approximate center of the spectrum (∼ 8.0 ppm), which is indicative of an unfolded or denatured protein.[40] In contrast, the 2D ^{1}H-^{15}N HSQC spectra for the oxidized form of DJ-1 showed a band of peaks around 8 ppm at 37°C, which intensified as the temperature was lowered to 5°C (Figure 4d–f and S3). Like the 2D ^{1}H-^{15}N HSQC spectrum for the reduced form, 134 peaks could be reliably assigned at 37°C for the oxidized form of DJ-1. However, the dramatic loss of peaks seen with the reduced form of DJ-1 as the temperature was lowered was not as prominent for the oxidized form of DJ-1. At 5°C, 62 of 180 residues could still be reliably assigned. The prevalence of the two spectral states for the oxidized form of DJ-1, band of peaks around 8 ppm and the assignable peaks, increased with lower temperatures.

A comparison of the temperature-dependent 2D ^{1}H-^{15}N HSQC spectra (Figure 4g–i and S4) for the over-oxidized form of DJ-1 suggested a significant collapse in chemical shift dispersion that was expected for a properly folded protein. While there was still a lack of chemical shift dispersion at 37°C, the amount of presumably denatured DJ-1 was not as dramatic at physiological temperature as it was at lower temperatures. A decrease in temperature caused a further decrease in chemical shift dispersion, an increase in peak broadening, and a loss in the number of detectable and assignable peaks for the over-oxidized form of DJ-1. In fact, the over-oxidized form of DJ-1 behaved quite differently from the reduced and oxidized forms as the temperature was lowered. At 37°C, 120 of the 180 peaks could be reliably assigned in the 2D ^{1}H-^{15}N HSQC spectrum for the over-oxidized form of DJ-1. This is lower than either the reduced or oxidized forms and can be partly attributed to severe peak overlap and the additional peaks centered around 8 ppm. At 5°C, only 25 peaks were assigned in the 2D ^{1}H-^{15}N HSQC spectrum for the over-oxidized form of DJ-1, which followed a similar trend as the reduced form of DJ-1. Peak assignments were challenging and potentially unreliable for the over-oxidized form due to severe peak broadening and overlap, especially around 8 ppm.

Importantly, the temperature-dependent effects on the 2D ^{1}H-^{15}N HSQC spectra for the over-oxidized form of DJ-1, though dramatic, were completely reversible. A 2D ^{1}H-^{15}N HSQC spectrum collected at room temperature right after obtaining the 5°C spectrum
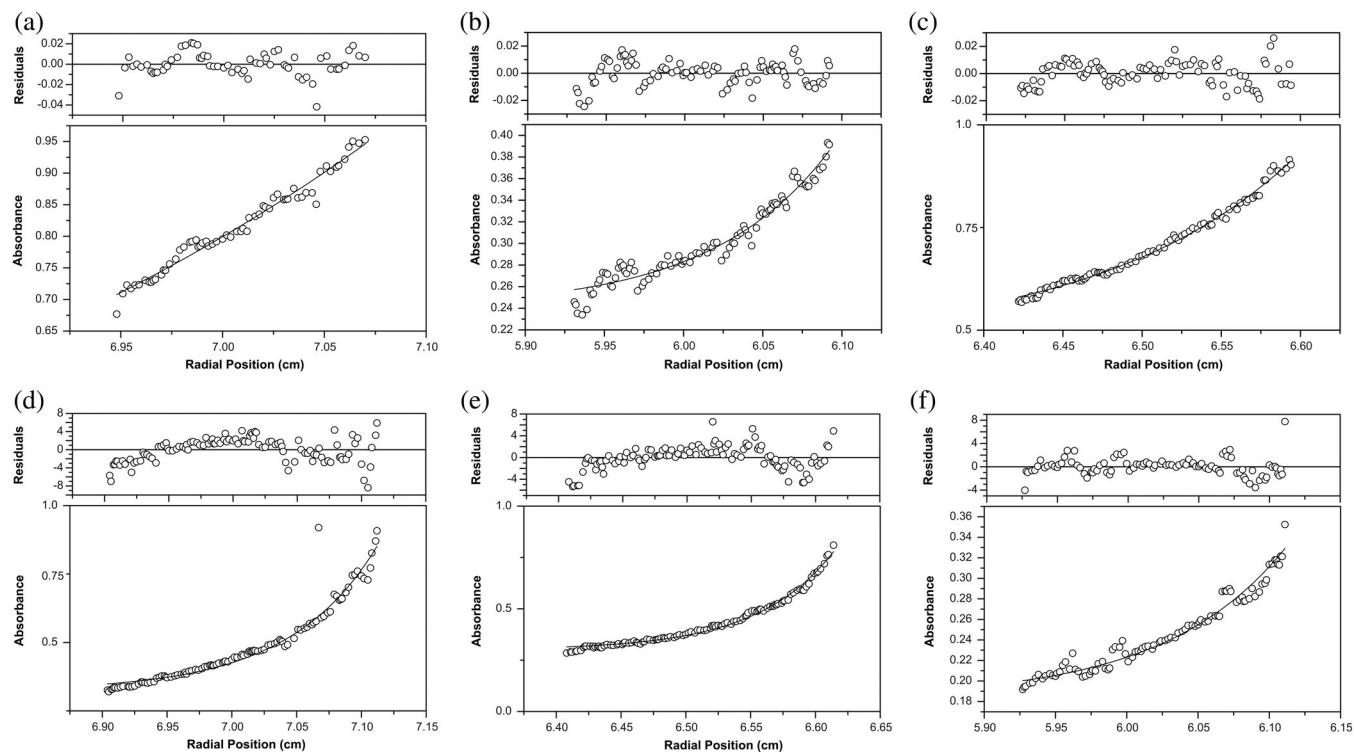
FIGURE 3 Representative AUC (*bottom*) fit and (*top*) residual plots of the (A, D) reduced, (B, E) oxidized, and (C, F) over-oxidized forms of DJ-1 at (a-c) 20°C and (d-f) 5°C.
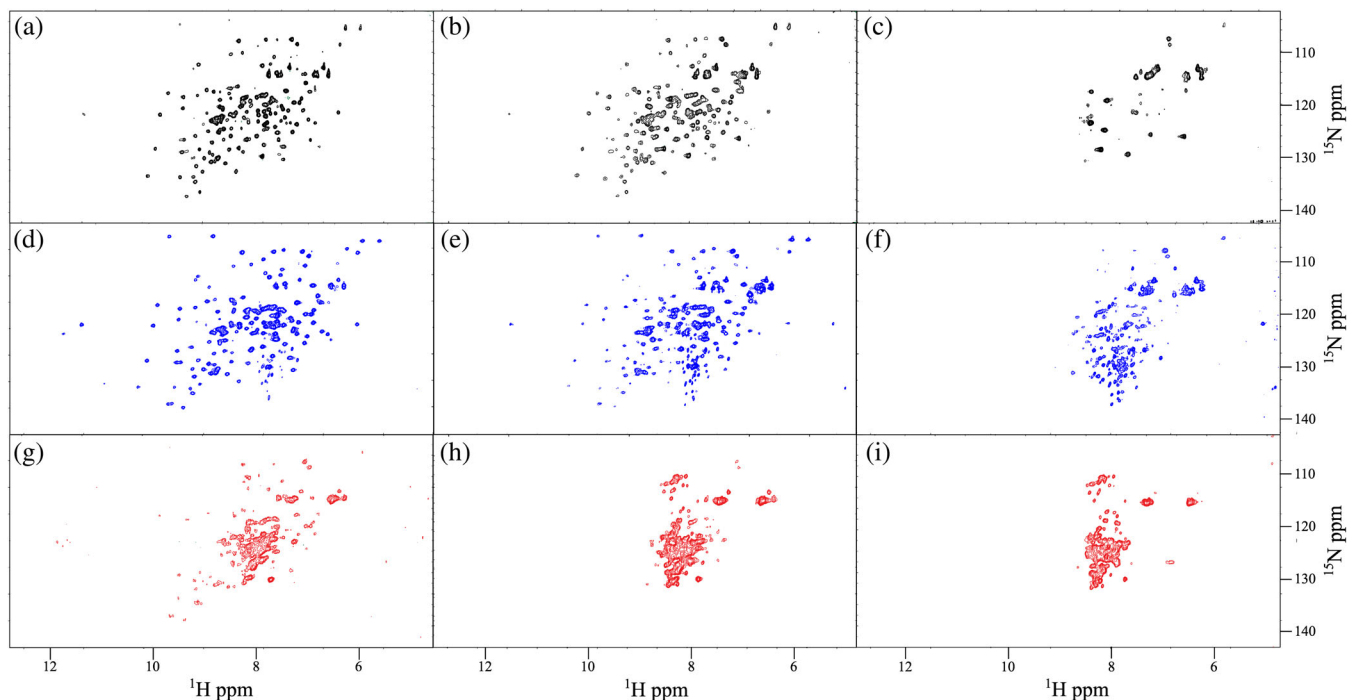
FIGURE 4 2D ^{1}H-^{15}N HSQC spectra of the reduced form of DJ-1 at (a) 37°C, (b) 20°C, and (c) 5°C, the oxidized form of DJ-1 at (d) 37°C, (e) 20°C, and (f) 5°C, and the over-oxidized form of DJ-1 at (g) 37°C, (h) 20°C, and (i) 5°C.

was completely consistent with the chemical shifts and assignments for the room temperature spectrum of the reduced form of DJ-1. The reversibility of this low-temperature-dependent aggregation-denaturation

phenomenon was also seen with the oxidized form of DJ-1. The unique features of the 5°C spectrum of the oxidized form of DJ-1 (e.g., the loss of chemical shift dispersion and the additional peaks

centered around 8 ppm) completely disappeared when the sample was heated back up to room temperature. A similar reversibility was observed for the reduced form of DJ-1.

3.5 | Temperature-dependent chemical shift and linewidth perturbations of the oxidative states of DJ-1

The CSPs of the reduced, oxidized and over-oxidized forms of DJ-1 were calculated relative to the previously reported backbone assignments (BMRB ID 17507) that were acquired at 25°C (Figure 5a and Table S3).[56] The annotated 2D ^{1}H-^{13}C HSQC for the reduced, oxidized, and over-oxidized forms of DJ-1 used to measure CSPs and linewidth changes are shown in Figures S2–S4. To clarify, CSPs were only reported for the assignable resonances at each temperature and

oxidative state. As expected, the CSPs increased linearly from 25°C at both higher and lower temperatures. For example, the reduced form of DJ-1 had average CSPs of 0.09 ± 0.04 and 0.04 ± 0.02 at 5°C and 37°C, respectively. These differences were statistically significant with a p-value <0.0001. In fact, a comparison of the average CSPs for the reduced form of DJ-1 at each temperature relative to the CSPs at 5°C were all statistically significant except for the average CSPs at 10°C (p-value 0.28). Notably, the average CSP at 37°C was only statistically different when compared to the CSPs at 5°C. Specifically, the average CSP at 5°C was almost double the average CSP at 37°C, suggesting a more dramatic structural change was occurring at lower temperatures. Surprisingly, the CSPs for the reduced form of DJ-1 exhibited a higher variability and a larger increase at lower temperatures relative to the oxidized and over-oxidized forms. This trend was reversed at higher temperatures.
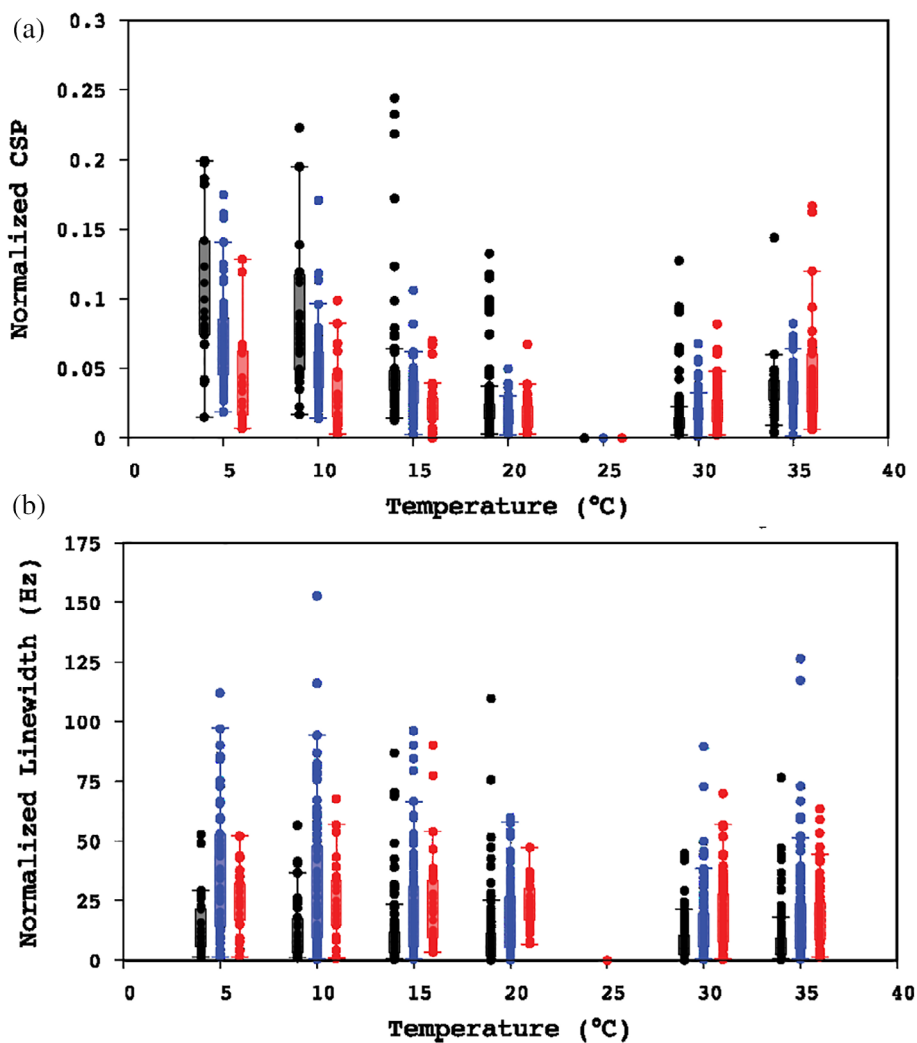
FIGURE 5 (a) Temperature-dependent CSPs for the DJ-1 oxidative states are plotted as box plots. The CSPs were calculated from the 2D ^{1}H-^{15}N HSQC spectra in Figure 4 and relative to the chemical shift assignments at 25°C (BMRB ID 17507).[56] The CSPs are colored black for the reduced, blue for the oxidized form, and red for the over-oxidized form of DJ-1. (b) Temperature-dependent linewidths for the DJ-1 oxidative states are plotted as box plots. The peak linewidths were calculated from the 2D ^{1}H-^{15}N HSQC spectra in Figure 4 and relative to the linewidths at 25°C. The linewidths are colored black for the reduced, blue for the oxidized form, and red for the over-oxidized form of DJ-1.

Inspection of the per-residue CSP values for the reduced form of DJ-1 at 37°C and 30°C identified one significant outlier corresponding to residue I52. The CSPs were 0.14 and 0.13 (p-value <0.05) at 37°C and 30°C, respectively. I52 is located at the DJ-1 dimer interface. At 20°C, T19 became a significant outlier, while E15 was a significant outlier at both 15°C and 10°C. These residues are also located at the dimer interface.

As the sample temperature was reduced, the oxidized form of DJ-1 behaved in a different manner relative to the reduced form. Again, the CSPs for the oxidized form of DJ-1 were statistically lower (p-values < 0.001) at all temperatures when compared to the reduced form (Figure 5a). It is also important to note that there were almost triple the number of assignable peaks in the oxidized form of DJ-1 relative to the reduced form at 5°C. Like the reduced form, there were several significant outliers in the per-residue CSPs. Specifically, residues I9, D189, A165, and L92 were outliers from 10°C to 37°C. But unlike the reduced form, only A165 was potentially involved in the dimer interface. The other residues were randomly located throughout the DJ-1 structure.

A further detailed analysis of the CSPs made it readily apparent that the over-oxidized structure responded differently to low temperatures relative to both the reduced and oxidized forms (Figure 5a). At 5°C, the over-oxidized form of DJ-1 had a lower average CSP of 0.04 ± 0.03 relative to both the reduced and oxidized forms of DJ-1. Like the reduced form of DJ-1, there were significantly less peaks in the 2D ^{1}H-^{15}N HSQC spectrum at 5°C that were reliably assigned. Only 21 peaks were assigned at 5°C compared to 120 assignments at 37°C. There were other notable differences in the 2D ^{1}H-^{15}N HSQC spectra for the over-oxidized form compared to the reduced and oxidized forms. For example, the average CSPs were statistically distinct between 37°C and 5°C for the reduced and oxidized forms. Conversely, the average CSPs for the over-oxidized form were statistically equivalent at 37°C (0.04 ± 0.03) and 5°C (0.04 ± 0.03). However, the CSPs at both 37°C and 5°C were statistically different from the CSPs at 20°C (p-value < 0.001).

The temperature-dependent changes in the 2D ^{1}H-^{15}N HSQC linewidths were also measured for the reduced, oxidized, and over-oxidized forms of DJ-1 (Table S3). As with the CSPs, the three DJ-1 oxidation states exhibited distinct temperature-dependent changes in the 2D ^{1}H-^{15}N HSQC linewidths. For the reduced form of DJ-1, the average normalized linewidths were less than 20 Hz at all temperatures (12.8 ± 8.6 at 5°C and 7.8 ± 8.7 Hz at 37°C), which was significantly below the oxidized and over-oxidized forms (Figure 5b). The linewidth differences were statistically insignificant between 5°C and 30°C. The only observable difference was between 5°C and 37°C. Again, the number of well-defined and assignable peaks in the 2D ^{1}H-^{15}N HSQC spectrum at 5°C was significantly less than at 37°C, which may underestimate the overall change in peak linewidths. For example, a few peaks at 20°C experienced severe line broadening, but these peaks were unassignable at 5°C and, thus, did not contribute to the overall change in the average linewidth.

In contrast, the average linewidth for the oxidized form of DJ-1 exhibited several unique temperature-dependent differences (Figure 5b).

First, the linewidths were much larger for the oxidized form, with values more than double that of the reduced form. For example, the average linewidth at 37°C in the oxidized form of DJ-1 was 20.2 ± 34.8 Hz compared to 7.8 ± 8.7 Hz for the reduced form. Unlike the reduced form of DJ-1, the average linewidth for the oxidized form of DJ-1 increased approximately linearly as the temperature decreased. Linewidths more than doubled to 43.0 ± 47.0 Hz at 5°C. The variability in linewidths exhibited a similar temperature-dependent trend. Again, unlike the reduced form, the oxidized form of DJ-1 exhibited similar increases in both the average linewidth and linewidth variability as the temperature was increased from 25°C to 37°C.

Like the oxidized form of DJ-1, the over-oxidized form had larger linewidths compared to the reduced form (Figure 5b). However, unlike the oxidized form that exhibited a linear increase in linewidths at every temperature, the over-oxidized form of DJ-1 had consistently large linewidths at all temperatures. In fact, the over-oxidized form had equal or larger linewidths than the oxidized form at higher temperatures (15°C to 37°C), but the oxidized form surpassed the oxidized form by 5°C. Interestingly, the over-oxidized form exhibited smaller standard deviations in linewidths compared to the oxidized form, especially at lower temperatures.

3.6 | MD simulations highlights the unusually low-temperature behavior of DJ-1

MD simulations were performed to gain insight into the dynamics of the reduced form of DJ-1 compared to the oxidized and over-oxidized forms. The recently determined parameters of SO_2^- and SO_3^- were used for the MD simulation of the oxidized and over-oxidized forms.[65] To the best of our knowledge, this is the first MD simulation that investigates these posttranslational modifications and their effect on protein dynamics. We performed standard MD simulations for the reduced, oxidized, and over-oxidized forms of DJ-1 at 5°C, 25°C and 37°C. Each simulation was run for 1 µs, which is consistent with prior literature values for comparing experimental and predicted order parameters (S^2).[68]

For reduced DJ-1, we observed a structural relaxation and the conformations sampled stayed within 2 Å RMSD from the starting structure throughout the simulation for all temperatures (Figure S5A). A similar behavior was observed for the oxidized form with a slight ~2.5 Å RMSD increase (Figure S5B). There was a modest increase in RMSD from the starting structure for the over-oxidized form of DJ-1 (Figure S5C) with an upward trend suggesting that with a longer simulation a structural transition may have been observed. Next, the iRed package was utilized to predict S^2 for each DJ-1 oxidative state to compare to our previously reported experimentally determined S^2 values.[52,53] In general, the simulated S^2 behaved as expected. A higher overall protein dynamic, smaller S^2 value, was observed as the oxidation state increased. In all three cases, the overall protein dynamic decreased as the temperature was lowered. Disappointingly, no agreement was observed between the experimental and simulated S^2 values (Figure 6) for the reduced ($R^2 = 0.08$), oxidized ($R^2 = 0.01$),
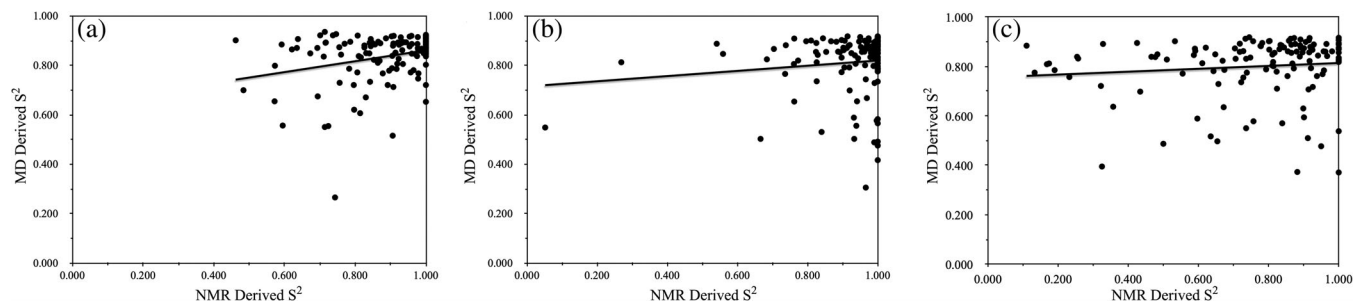
FIGURE 6 Scatter plots comparing the MD simulated order parameters (S^2) to the NMR derived S^2 values for the (a) reduced, (b) oxidized and (c) over-oxidized forms of the DJ-1 homodimer at 37°C. The best-fit lines are shown where the R^2 values are 0.08, 0.01, and 0.01 for the reduced, oxidized, and over-oxidized forms, respectively.

and over-oxidized ($R^2 = 0.01$) forms. This contrasts with previous comparisons between experimental and simulated S^2 values determined for other proteins using iRED that yielded good correlations.[68]

4 | DISCUSSION

While the cellular functions of DJ-1 have not been clearly defined, it is postulated to have roles related to the control of ROS and in response to oxidative stress.[21,30,31,38–45] Of course, oxidative stress has been identified as an important contributing factor to PD where ROS leads to the death of the dopaminergic neurons in the substantia nigra.[69] Thus, a loss in DJ-1 functional activity is believed to be a contributing factor to PD progression.[30] Numerous deletions and point mutations in DJ-1 have been identified in patients with PD (e.g., L166P, E163K, P158Δ, D149A, A104T, E64D, M26I, L10P, etc.) that led to a loss-of-function.[20,55,56,70–74] Some mutations disrupted DJ-1 dimerization (i.e., L10P and P158Δ) and denatured the protein (i.e., L166P), while other mutations had more subtle structural effects.[56,70–72,74] For example, the sulfinate or oxidized form (C106-SO$_2^-$) of DJ-1 is structurally similar to the WT protein (Figure 1).[46,55–57] Notably, the oxidized form of DJ-1 exhibits enhanced neuroprotective function and localization to the mitochondria,[75] while the over-oxidized form of DJ-1 is thought to be inactive and contribute to DJ-1 pathology,[46,48] and decreases DJ-1 structural stability.[65,73] Thus, some mutations or modifications to DJ-1 lead to a clear loss of structure and function, while others preserve a properly folded but biologically inactive protein. This is particularly intriguing when comparing the oxidized and over-oxidized forms of DJ-1. We have previously shown that the over-oxidation of DJ-1 greatly increased the dynamic instability at 37°C that likely leads to protein aggregation and precipitation.[52,53] This dynamic instability may explain the loss of function despite a structure similar to WT DJ-1.[46,55–57] We investigated the impact of temperature on DJ-1 to further explore the role dynamics and protein aggregation has on DJ-1 cellular activity. NMR spectroscopy, CD, AUC, and MD simulations were used to characterize changes in the reduced, oxidized and over-oxidized forms of DJ-1 as a function of temperature, which is summarized in Figure 7.

The AUC experiments suggested temperature and oxidation levels induced distinct oligomeric or aggregation states for DJ-1 (Figure 3 and Table 1). Specifically, the number of macromolecular interactions increased as C106 was oxidized and as the temperature decreased. At 20°C and in the presence of DTT, the reduced form of DJ-1 had an apparent molecular-weight of 20 kDa, which is consistent with a monomer. DTT was added to the AUC sample to ensure a reduced form of DJ-1, and the observed monomer form of DJ-1 is simply an artifact of this sample condition. It is well established that the WT and reduced form of DJ-1 is a dimer.[22,55,65,76]

Conversely, the oxidized and over-oxidized forms of DJ-1 exhibited apparent molecular-weights of 63 and 104 kDa, oligomers consisting of 3 and 5 monomers, respectively. Unexpectedly, all three DJ-1 oxidative states increased, within error, to nearly the same apparent mass (~104 to 138 kDA) or oligomeric state (5 to 7 monomeric units) as the temperature was lowered to 5°C. This suggests that the three oxidative states of DJ-1 behaved relatively similar at low temperatures and formed large molecular-weight complexes. Interestingly, these 5°C oligomers were like the over-oxidized form at 20°C.

The differences in the molecular-weights of the three oxidative states at 20°C further supports the premise that the over-oxidized form is less stable and more prone to aggregation-like interactions. The AUC results also suggest the reduced and oxidized forms of DJ-1 behave differently below physiological temperature and form aggregates. Importantly, since the CD data (Figure 2) indicated the secondary structure was maintained for the three different oxidative states at 5°C, the oligomeric forms indicated by the AUC data are likely not comprised of completely denatured aggregates.

Similarly, the qualitative analysis of the 2D ^{1}H-^{15}N HSQC spectra for the reduced, oxidized, and over-oxidized forms of DJ-1 showed three distinctly different behaviors as the temperature was decreased (Figure 7). As seen in Figures 4 and 5, S2–S4 and Table S3 there were significant differences in the number of assignable peaks, the dispersion of chemical shifts, and the changes in CSPs and linewidths between the three oxidative states as a function of temperature. The temperature-dependent transitions in the 2D ^{1}H-^{13}C HSQC spectra paralleled the relative order of structural stability of the reduced (high), oxidized (moderate), and over-oxidized (low) forms of DJ-1, respectively.
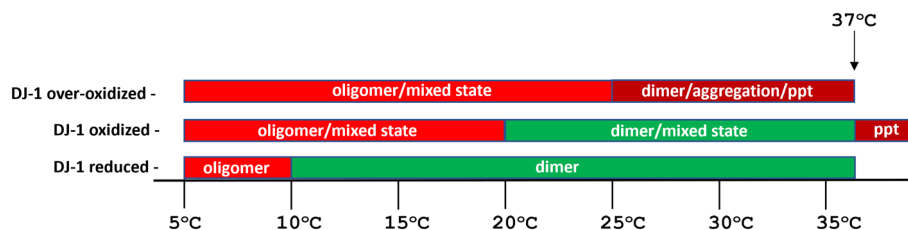
FIGURE 7 Schematic diagram of the structural changes in DJ-1 resulting from low temperature and oxidation state. The protein precipitation block was added to the end of the DJ-1 oxidized row to highlight that the oxidized form is less stable than the reduced form. ppt: protein precipitation.

The 2D ^{1}H-^{13}C HSQC spectra for the reduced form of DJ-1 were consistent with a properly folded protein with minimal CSPs and line-width changes from 20°C to 37°C. The spectra essentially collapsed at 5°C and 10°C and there were few observable peaks still consistent with the properly folded DJ-1 dimer at 25°C. The remaining number of peaks was significantly less than both oxidized states with significantly larger CSPs and a higher variance in peak intensities (Table S3). These residues were located at the dimer interface. Overall, the 2D ^{1}H-^{13}C HSQC spectra suggested a dramatic structural change was occurring at the dimer interface at low temperature (10°C to 5°C) that was more pronounced for the reduced form relative to the oxidized states. Essentially, the reduced form of DJ-1 was more stable than the oxidized states and simply required a lower temperature to undergo a cold-induced aggregation. There was no visible evidence of protein denaturation or precipitation.

A similar temperature-dependent trend was observed in the 2D ^{1}H-^{13}C HSQC spectra for the oxidized form of DJ-1. This was consistent with previous studies that indicated the reduced and oxidized forms of DJ-1 behave very similarly at physiological temperature, while the over-oxidized form was less stable at 37°C.[39] Nevertheless, there were still notable differences between the reduced and oxidized spectra at 5°C and 10°C. A larger number of peaks were observed in the spectra for the oxidized form of DJ-1 and most of these detectable peaks were consistent with a denatured protein. Importantly, this band of peaks was also present in the spectra for the oxidized form at higher temperatures. Furthermore, the oxidized form exhibited a larger relative increase in linewidths relative to both the reduced and over-oxidized forms. Also, the residues in the oxidized form with the largest low-temperature CSPs were randomly distributed throughout the DJ-1 structure and not located in the dimer interface like the reduced form. Thus, instead of the structural changes being restricted to the dimer interface, it appears a global structural change was occurring to the oxidized form of DJ-1 as the temperature was lowered. The cluster of peaks at 8 ppm and the ability to assign a larger majority of the remaining peaks suggests the presence of two distinct states: (1) a partially folded state and (2) a partially denatured state for the oxidized form of DJ-1. Overall, the 2D ^{1}H-^{13}C HSQC spectra for the oxidized form suggests the primary structural change was a cold-induced aggregation. There was no evidence of protein precipitation.

The temperature-dependent changes in the 2D ^{1}H-^{13}C HSQC spectra for the over-oxidized form of DJ-1 were more pronounced

and occurred quickly as the temperature was decreased. The NMR spectra at 30°C and 37°C only partially resembled the 2D ^{1}H-^{13}C HSQC spectra for a properly folded WT DJ-1 dimer. The band of peaks around 8 ppm that are consistent with a denatured protein was more intense compared to the oxidized form. Again, the over-oxidized form exhibited the smallest temperature-dependent CSPs while having consistently broad linewidths. Reducing the temperature to only 25°C resulted in a dramatic collapse in the 2D ^{1}H-^{13}C HSQC spectra. The nearly complete loss of chemical shift dispersion and the presence of broad peaks is consistent with a denatured protein. In fact, it was difficult to discern individual peaks in the over-oxidized spectra. Again, the presence of some assignable peaks suggested that there were multiple conformations of DJ-1 at each temperature: (1) a partially folded and structurally stable conformation with assignable NMR peaks and (2) a structurally unstable potentially aggregated conformation with unassigned peaks. Again, these states occurred sooner than both the reduced and oxidized forms of DJ-1. While the results for the over-oxidized form of DJ-1 were expected, the stark differences seen in the NMR spectra for the reduced and oxidized form at 5°C were surprising. The partial or complete collapse of chemical shift dispersion and the dramatic lose in detectable peaks as the temperature was lowered suggested both a cold-induced denaturation and protein aggregation had occurred.

The low stability of the over-oxidized form of DJ-1 was further evident by the fact that this oligomerization began at only 25°C. Again, consistent with the AUC data, which showed a high oligomer state at 20°C with no change as the temperature was reduced to 5°C. In essence, the over-oxidized form of DJ-1 was quickly destabilized with small increases or decreases in temperature that produced an aggregated and inactive protein. Conversely, both the NMR spectra down to 15°C and the AUC data at 20°C for the reduced form of DJ-1 suggested a properly folded protein that was not aggregated. The behavior of the oxidized form of DJ-1 appeared to fall between the reduced and over-oxidized forms. Both the oxidized and over-oxidized forms showed a mixture of both properly folded and denatured protein that increased as the temperature was decreased. The amount of denatured protein was more pronounced in the over-oxidized form and absent in the reduced form of DJ-1.

The CD data (Figure 2) may appear to contradict the NMR data since it predicts a secondary structure composition comparable to the WT DJ-1 X-ray structure that does not change with a decrease in

temperature or oxidation state. This could suggest the protein denaturation and/or aggregation process was concentration dependent since the CD was obtained at a significantly lower concentration than the NMR spectra. Alternatively, since the NMR and AUC data suggested a complex mixture of states, residual secondary structures, particularly α-helices, may still be present in a partially denatured or molten globule-type structure. The CD does not differentiate between secondary structures that are present in a properly folded, aggregated, or partially denatured protein. Thus, the CD data suggests the total amount of secondary structure was only minimally affected by the oxidation state or by a lower temperature.

The MD simulations indicated that the reduced, oxidized, and over-oxidized forms of DJ-1 may be exhibiting dynamic differences as the temperature was varied (Figure S6). Specifically, as C106 was oxidized, the relative internal motions of DJ-1 increased. At low temperatures, the simulated S^2 values were significantly higher than observed at physiological temperature regardless of the oxidation state. This is consistent with a general expectation that protein dynamics decreases linearly with temperature,[77,78] but was completely inconsistent with the dramatic cold-induced aggregation and denaturation observed by NMR and AUC. A direct comparison of the order parameters calculated at 37°C showed no correlation between the experimental and simulated S^2 values for the three oxidative states of DJ-1 (Figure 6). The inability of the MD simulation to replicate the order parameters for the DJ-1 oxidative states at 37°C and the cold-induced changes to the protein suggests there are some large conformational changes (ms or longer time frame) that would require a significantly longer MD simulation time to properly reproduce these DJ-1 structural changes. Simply, DJ-1 is quite unusual and does not behave as an "ordinary" protein as predicted by the relatively short MD simulations.

Overall, all three oxidative states of DJ-1 appeared to form aggregates or oligomers as the temperature was decreased to 5°C (Figure 7). It is also important to note that these dramatic changes were surprisingly completely reversible. To be clear, there was no observable cold-induced precipitation of either of the three DJ-1 oxidation states. This reversible cold denaturation and aggregation phenomenon has not been previously characterized in DJ-1, and to the best of our knowledge in other proteins. Consistent with our temperature-dependent aggregation findings was the observation by Kobayashi et al. that the oxidized form of DJ-1 polymerized (MW 60 to 250 kDa) based on disulfide bonds and other noncovalent and covalent interactions. Importantly, these DJ-1 polymers were recovered from *E. coli* cells over-expressing DJ-1 after treatment with H_2O_2; the polymers could be reversed by a reducing agent. Similarly, high molecular-weight or polymer forms of DJ-1 (> 2000 kDa) have been detected in brain tissues and erythrocytes from human PD patients,[79–82] and oxidized DJ-1 has been shown to form soluble β-sheet aggregates.[82,83]

Multiple studies of WT DJ-1 have indicated the protein elutes as a dimer from a size exclusion column at 4°C, which differs from our AUC and NMR aggregation observation at 5°C.[25,84] It is well established that the natural state of DJ-1 is a homodimer,[22,55,65,76] therefore; the contradictory observation of a low-temperature oligomer-dimer state for DJ-1 suggests the oligomeric state derives from weak interactions where the equilibrium is easily shifted to the preferred dimer conformation. This proposition is supported by several observations that include the reversibility of the low-temperature DJ-1 aggregates-oligomers, the mixed structural state of these aggregates that contain remnants of the WT DJ-1 dimer, and the general knowledge that experimental conditions (concentration, buffer, ionic strength, pH, etc.) affect oligomer equilibria. Of course, size exclusion chromatography (SEC) can produce unreliable molecular-weight calculations if the protein complex interacts with the column matrix, if the complex is non-spherical (like the soluble β-sheet aggregates),[82,83] or the complex exchange rate is fast and the binding affinity is low (as suggested by reversible aggregates). In all of these cases, SEC would be untrustworthy and yield a lower molecular-weight than the true value for the oligomer.[85]

Protein aggregation and denaturation is typically irreversible. Thus, the ramifications of reversible DJ-1 aggregate to its role in PD is potentially high. Taken together, these DJ-1 structural findings provide further support to our previous studies[52–54] and to other studies that suggests a dynamic instability of DJ-1 occurs due to oxidation or mutation, which leads to a loss of function from denaturation and/or aggregation.[53] Our results also shed new insights on the structure and stability differences between the reduced and oxidized forms of DJ-1. The relative decrease in the structural stability of the oxidized form of DJ-1 may be relevant to its cytoprotection role against oxidative stress.

5 | CONCLUSION

The loss of function of the human protein DJ-1 has been associated with PD progression. PD is caused by the death of dopaminergic neurons in the substania nigra, which results from a complex combination of oxidative stress, protein aggregation, and the formation of Lewy bodies. While several cellular functions have been attributed to DJ-1, its cytoprotection against oxidative stress and its control of ROS appear important to PD. C106 is a highly conserved residue and is a key regulator of the cytoprotective role of DJ-1 where the over-oxidation of C106 leads to dynamic instability, protein aggregation, and a loss of function for DJ-1. Herein, we employed NMR spectroscopy, AUC sedimentation equilibrium experiments, CD, and MD simulation to monitor the change in DJ-1 structural stability as a function of oxidation state and temperature (Figure 7). While the low-temperature studies do not have a direct physiological connection, it does offer invaluable insights into the unique structural and dynamic behavior of DJ-1 that is relevant to PD progression. Low-temperature experiments also provided a valuable tool to further dissect the different behaviors of the DJ-1 oxidative states. For all three oxidative states, lowering the temperature resulted in a cold-induced aggregation, which has not been previously observed for DJ-1. Surprisingly, the cold-induced structural changes were completely reversible. There was no detectable protein precipitation. Both the oxidized and over-oxidized states included the presence of denatured protein that was observable at 37°C and increased as the temperature was lowered.

There was no evidence of denatured protein for the reduced form of DJ-1. The over-oxidized state of DJ-1 exhibited the lowest overall stability that resulted in protein aggregation and denaturation at both higher and lower temperatures. The temperature-dependent behavior of the oxidized form fell between the reduced and over-oxidized form. Overall, the dramatic changes in the strucutral stability of DJ-1 as a function of oxidative state is relent to its role in PD and its functional response to oxidative stress.

AUTHOR CONTRIBUTIONS

Tessa Andrews prepared samples performed the experiments and analyzed the data. Javier Seravallic assisted with the AUC sedimentation equilibrium and mass spectrometry experiments. Robert Powers conceived the project. Tessa Andrews and Robert Powers wrote and edited the manuscript.

ACKNOWLEDGMENTS

CONFLICT OF INTEREST

The authors declare no competing interests.

DATA AVAILABILITY STATEMENT

The data that support the findings of this study are available from the corresponding author upon reasonable request.

ORCID

Robert Powers https://orcid.org/0000-0001-9948-6837

REFERENCES

[1] C. M. Dobson, *Nature* **2003**, *426*, 884.

[2] C. Anfinsen, *B.* **1973**, *181*, 223.

[3] F. Pucci, M. Rooman, *J. Biomol. Struct. Dyn.* **2016**, *34*, 1132.

[4] Y. Yang, J. Zhao, L. Zeng, M. Vihinen, *Int. J. Mol. Sci.* **2022**, *23*, 10798.

[5] F. Pucci, R. Bourgeas, M. Rooman, *J. Phys. Chem. Ref. Data* **2016**, *45*, 023104.

[6] A. D. Robertson, K. P. Murphy, *Chem. Rev.* **1997**, *97*, 1251.

[7] T. Niwa, B.-W. Ying, K. Saito, W. Z. Jin, S. Takada, T. Ueda, H. Taguchi, *Proc. Natl. Acad. Sci. U.S.A* **2009**, *106*, 4201.

[8] M. Gonzalez-Garcia, G. Fusco, A. De Simone, *Front. Cell Dev. Biol.* **2021**, *9*, 642623.

[9] R. Rosenzweig, N. B. Nillegoda, M. P. Mayer, B. Bukau, *Nat. Rev. Mol. Cell Biol.* **2019**, *20*, 665.

[10] H. Kubota, *J. Biochem.* **2009**, *146*, 609.

[11] P. L. Privalov, *Crit. Rev. Biochem. Mol. Biol.* **1990**, *25*, 281.

[12] D. Sanfelice, P. A. Temussi, *Biophys. Chem.* **2016**, *208*, 4.

[13] C. Soto, S. Pritzkow, *Nat. Neurosci.* **2018**, *21*, 1332.

[14] D. T. Dexter, P. Jenner, *Free Radical Biol. Med.* **2013**, *62*, 132.

[15] W. Dauer, S. Przedborski, *Neuron* **2003**, *39*, 889.

[16] O. M. A. El-Agnaf, G. B. Irvine, *J. Struct. Biol.* **2000**, *130*, 300.

[17] K. Nuytemans, J. Theuns, M. Cruts, C. Van Broeckhoven, *Hum. Mutat.* **2010**, *31*, 763.

[18] D. Nagakubo, T. Taira, H. Kitaura, M. Ikeda, K. Tamai, S. M. M. Iguchi-Ariga, H. Ariga, *Biochem. Biophys. Res. Commun.* **1997**, *231*, 509.

[19] V. Bonifati, P. Rizzu, M. J. van Baren, O. Schaap, G. J. Breedveld, E. Krieger, M. C. J. Dekker, F. Squitieri, P. Ibanez, M. Joosse, J. W. van Dongen, N. Vanacore, J. C. van Swieten, A. Brice, G. Meco, C. M. van Duijn, B. A. Oostra, P. Heutink, *Science (Washington, DC, U. S.)* **2003**, *299*, 256.

[20] P. J. Kahle, J. Waak, T. Gasser, *Free Radical Biol. Med.* **2009**, *47*, 1354.

[21] A. Biosa, F. Sandrelli, M. Beltramini, E. Greggio, L. Bubacco, M. Bisaglia, *Neurobiol. Dis.* **2017**, *108*, 65.

[22] Q. Huai, Y. Sun, H. Wang, L.-S. Chin, L. Li, H. Robinson, H. Ke, *FEBS Lett.* **2003**, *549*, 171.

[23] X. Tao, L. Tong, *J. Biol. Chem.* **2003**, *278*, 31372.

[24] J.-F. Trempe, E. A. Fon, *Front. Neurodegener.* **2013**, *4*, 1.

[25] M. A. Wilson, J. L. Collins, Y. Hod, D. Ringe, G. A. Petsko, *Proc. Natl. Acad. Sci. U. S. A* **2003**, *100*, 9256.

[26] R. Bandopadhyay, A. E. Kingsbury, M. R. Cookson, A. R. Reid, I. M. Evans, A. D. Hope, A. M. Pittman, R. Lashley, R. Canet-Aviles, D. W. Miller, C. McLendon, C. Strand, A. J. Leonard, P. M. Abou-Sleiman, D. G. Healy, H. Ariga, N. W. Wood, R. De Silva, T. Revesz, J. A. Hardy, A. J. Lees, *Brain* **2004**, *127*, 420.

[27] S. Bandyopadhyay, M. R. Cookson, *BMC Evol. Biol.* **2004**, *4*, 6.

[28] N. Smith, M. A. Wilson, *Adv. Exp. Med. Biol.* **2017**, *1037*, 5.

[29] J. Waak, S. S. Weber, K. Goerner, C. Schall, H. Ichijo, T. Stehle, P. J. Kahle, *J. Biol. Chem.* **2009**, *284*, 14245.

[30] H. Ariga, K. Takahashi-Niki, I. Kato, H. Maita, T. Niki, S. M. Iguchi-Ariga, *Oxid. Med. Cell. Longev.* **2013**, *2013*, 683920.

[31] T. Taira, Y. Saito, T. Niki, S. M. M. Iguchi-Ariga, K. Takahashi, H. Ariga, *EMBO Rep.* **2004**, *5*, 213.

[32] K. Takahashi-Niki, H. Ariga, T. Niki, S. M. M. Iguchi-Ariga, *Adv. Exp. Med. Biol.* **2017**, *1037*, 89.

[33] R. Wu, X.-M. Liu, J.-G. Sun, H. Chen, J. Ma, M. Dong, S. Peng, J.-Q. Wang, J.-Q. Ding, D.-H. Li, J. R. Speakman, G. Ning, W. Jin, Z. Yuan, *Cell Discov.* **2017**, *3*, 16054.

[34] S.-J. Kim, Y.-J. Park, I.-Y. Hwang, M. B. H. Youdim, K.-S. Park, Y. J. Oh, *Free Radical Biol. Med.* **2012**, *53*, 936.

[35] C. Maita, H. Maita, S. M. M. Iguchi-Ariga, H. Ariga, *PLoS One* **2013**, *8*, e54087.

[36] T. Yanagida, J. Tsushima, Y. Kitamura, D. Yanagisawa, K. Takata, T. Shibaike, A. Yamamoto, T. Taniguchi, H. Yasui, T. Taira, S. Morikawa, T. Inubushi, I. Tooyama, H. Ariga, *Oxid. Med. Cell. Longevity* **2009**, *2*, 36.

[37] R. H. Kim, P. D. Smith, H. Aleyasin, S. Hayley, M. P. Mount, S. Pownall, A. Wakeham, A. J. You-Ten, S. K. Kalia, P. Horne, D. Westaway, A. M. Lozano, H. Anisman, D. S. Park, T. W. Mak, *Proc. Natl. Acad. Sci. U. S. A.* **2005**, *102*, 5215.

[38] H. Gao, W. Yang, Z. Qi, L. Lu, C. Duan, C. Zhao, H. Yang, *J. Mol. Biol.* **2012**, *423*, 232.

[39] J.-Y. Im, K.-W. Lee, E. Junn, M. M. Mouradian, *Neurosci. Res. (Shannon, Irel)* **2010**, *67*, 203.

[40] J.-Y. Im, K.-W. Lee, J.-M. Woo, E. Junn, M. M. Mouradian, *Hum. Mol. Genet.* **2012**, *21*, 3013.

[41] E. Junn, H. Taniguchi, B. S. Jeong, X. Zhao, H. Ichijo, M. M. Mouradian, *Proc. Natl. Acad. Sci. U. S. A* **2005**, *102*, 9691.

[42] D. Ottolini, T. Cali, A. Negro, M. Brini, *Hum. Mol. Genet.* **2013**, *22*, 2152.

[43] Z. Wang, J. Liu, S. Chen, Y. Wang, L. Cao, Y. Zhang, W. Kang, H. Li, Y. Gui, S. Chen, J. Ding, *Ann. Neurol.* **2011**, *70*, 591.

[44] R. H. Kim, M. Peters, Y. Jang, W. Shi, M. Pintilie, G. C. Fletcher, C. DeLuca, J. Liepa, L. Zhou, B. Snow, R. C. Binari, A. S. Manoukian, M. R. Bray, F.-F. Liu, M.-S. Tsao, T. W. Mak, *Cancer Cell* **2005**, *7*, 263.

[45] H. Ren, K. Fu, C. Mu, B. Li, D. Wang, G. Wang, *Cancer Lett.* **2010**, *297*, 101.

[46] R. M. Canet-Avilés, M. A. Wilson, D. W. Miller, R. Ahmad, C. McLendon, S. Bandyopadhyay, M. J. Baptista, D. Ringe, G. A. Petsko, M. R. Cookson, *Proc. Natl. Acad. Sci. U. S. A* **2004**, *101*, 9103.

[47] T. Kinumi, J. Kimata, T. Taira, H. Ariga, E. Niki, *Biochem. Biophys. Res. Commun.* **2004**, *317*, 722.

[48] M. A. Wilson, *Antioxid. Redox Signaling* **2011**, *15*, 111.

[49] C. A. Davie, *Br. Med. Bullet.* **2008**, *86*, 109.

[50] S. Lesage, A. Brice, *Hum. Mol. Genet.* **2009**, *18*, 48.

[51] J. Choi, M. C. Sullards, J. A. Olzmann, H. D. Rees, S. T. Weintraub, D. E. Bostwick, M. Gearing, A. I. Levey, L. S. Chin, L. Li, *J. Biol. Chem.* **2006**, *281*, 10816.

[52] K. Bahmed, S. Boukhenouna, L. Karim, T. Andrews, J. Lin, R. Powers, M. A. Wilson, C.-R. Lin, E. Messier, N. Reisdorph, R. L. Powell, H.-Y. Tang, R. J. Mason, G. J. Criner, B. Kosmider, *Cell Death Disease* **2019**, *10*, 638.

[53] J. Catazaro, T. Andrews, N. M. Milkovic, J. Lin, A. J. Lowe, M. A. Wilson, R. Powers, *Anal. Biochem.* **2018**, *542*, 24.

[54] N. M. Milkovic, J. Catazaro, J. Lin, S. Halouska, J. L. Kizziah, S. Basiaga, R. L. Cerny, R. Powers, M. A. Wilson, *Protein Sci.* **2015**, *24*, 1671.

[55] F. E. Herrera, S. Zucchelli, A. Jezierska, Z. S. Lavina, S. Gustincich, P. Carloni, *J. Biol. Chem.* **2007**, *282*, 24905.

[56] G. Malgieri, D. Eliezer, *Protein Sci.* **2008**, *17*, 855.

[57] S. Tashiro, J. M. M. Caaveiro, C.-X. Wu, Q. Q. Hoang, K. Tsumoto, *Biochemistry* **2014**, *53*, 2218.

[58] J. Prahlad, D. N. Hauser, N. M. Milkovic, M. R. Cookson, M. A. Wilson, *J. Neurochem.* **2014**, *130*, 839.

[59] C. Wiedemann, P. Bellstedt, M. Goerlach, *Bioinformatics* **2013**, *29*, 1750.

[60] P. H. Brown, A. Balbo, P. Schuck, *Eur. Biophys. J.* **2009**, *38*, 1079.

[61] F. Delaglio, S. Grzesiek, G. W. Vuister, G. Zhu, J. Pfeifer, A. Bax, *J. Biomol. NMR* **1995**, *6*, 227.

[62] W. Lee, M. Tonelli, J. L. Markley, *Bioinformatics* **2015**, *31*, 1325.

[63] D. Van Der Spoel, E. Lindahl, B. Hess, G. Groenhof, A. E. Mark, H. J. C. Berendsen, *J. Comput. Chem.* **2005**, *26*, 1701.

[64] A. C. Witt, M. Lakshminarasimhan, B. C. Remington, S. Hasim, E. Pozharski, M. A. Wilson, *Biochemistry* **2008**, *47*, 7430.

[65] R. Kiss, M. Zhu, B. Jójárt, A. Czajlik, K. Solti, B. Fórizs, É. Nagy, F. Zsila, T. Beke-Somfai, G. Tóth, *Biochim. Biophys. Acta – Gen. Subj.* **1861**, *2017*, 2619.

[66] J. J. Prompers, R. Brüschweiler, *J. Am. Chem. Soc.* **2002**, *124*, 4522.

[67] I. Karaman, D. L. S. Ferreira, C. L. Boulangé, M. R. Kaluarachchi, D. Herrington, A. C. Dona, R. Castagné, A. Moayyeri, B. Lehne, M. Loh, P. S. de Vries, A. Dehghan, O. H. Franco, A. Hofman, E. Evangelou, I. Tzoulaki, P. Elliott, J. C. Lindon, T. M. D. Ebbels, *J. Proteome Res.* **2016**, *15*, 4188.

[68] H. L. Zwibel, J. Smrtka, *Am. J. Manag. Care* **2011**, 17 Suppl 5 Improving, S139-145, *17 Suppl 5 Improving*, S139.

[69] V. Dias, E. Junn, M. M. Mouradian, *J. Parkinsons Dis.* **2013**, *3*, 461.

[70] C. P. Ramsey, B. I. Giasson, *J. Neurosci. Res.* **2010**, *88*, 3111.

[71] M. Repici, K. R. Straatman, N. Balduccio, F. J. Enguita, T. F. Outeiro, F. Giorgini, *J. Molec. Med.* **2013**, *91*, 599.

[72] D. W. Miller, R. Ahmad, S. Hague, M. J. Baptista, R. Canet-Aviles, C. McLendon, D. M. Carter, P.-P. Zhu, J. Stadler, J. Chandran, G. R. Klinefelter, C. Blackstone, M. R. Cookson, *J. Biol. Chem.* **2003**, *278*, 36588.

[73] J. D. Hulleman, H. Mirzaei, E. Guigard, K. L. Taylor, S. S. Ray, C. M. Kay, F. E. Regnier, J.-C. Rochet, *Biochemistry* **2007**, *46*, 5776.

[74] D. J. Moore, L. Zhang, T. M. Dawson, V. L. Dawson, *J. Neurochem.* **2003**, *87*, 1558.

[75] E. Junn, W. H. Jang, X. Zhao, B. S. Jeong, M. M. Mouradian, *J. Neurosci. Res.* **2009**, *87*, 123.

[76] K. Honbou, N. N. Suzuki, M. Horiuchi, T. Niki, T. Taira, H. Ariga, F. Inagaki, *J. Biol. Chem.* **2003**, *278*, 31380.

[77] X.-j. Song, P. F. Flynn, K. A. Sharp, A. J. Wand, *Biophys. J.* **2007**, *92*, L43.

[78] T. Wang, S. Cai, E. R. P. Zuiderweg, *J. Am. Chem. Soc.* **2003**, *125*, 8639.

[79] M. C. Meulener, C. L. Graves, D. M. Sampathu, C. E. Armstrong-Gold, N. M. Bonini, B. I. Giasson, *J. Neurochem.* **2005**, *93*, 1524.

[80] S. Baulac, M. J. LaVoie, J. Strahle, M. G. Schlossmacher, W. Xia, *Mol. Cell. Neurosci.* **2004**, *27*, 236.

[81] H. Nural, P. He, T. Beach, L. Sue, W. Xia, Y. Shen, *Molec. Neurodegener.* **2009**, *4*, 1.

[82] Y. Saito, Y. Akazawa-Ogawa, A. Matsumura, K. Saigoh, S. Itoh, K. Sutou, M. Kobayashi, Y. Mita, M. Shichiri, S. Hisahara, Y. Hara, H. Fujimura, H. Takamatsu, Y. Hagihara, Y. Yoshida, T. Hamakubo, S. Kusunoki, S. Shimohama, N. Noguchi, *Sci. Rep.* **2016**, *6*, 30793.

[83] K. Solti, W.-L. Kuan, B. Fórizs, G. Kustos, J. Mihály, Z. Varga, B. Herberth, É. Moravcsik, R. Kiss, M. Kárpáti, A. Mikes, Y. Zhao, T. Imre, J.-C. Rochet, F. Aigbirhio, C. H. Williams-Gray, R. A. Barker, G. Tóth, *Neurobiol. Dis.* **2020**, *134*, 104629.

[84] J. A. Olzmann, K. Brown, K. D. Wilkinson, H. D. Rees, Q. Huai, H. Ke, A. I. Levey, L. Li, L.-S. Chin, *J. Biol. Chem.* **2004**, *279*, 8506.

[85] T. R. Dafforn, *Acta Crystallogr, Sect D: Biol Crystallogr* **2007**, *D63*, 17.

SUPPORTING INFORMATION

Additional supporting information can be found online in the Supporting Information section at the end of this article.